Conf-921206--5

PNL-SA--21027

DE93 005095



# EFFECTS OF AIR OXIDATION OF THE DISSOLUTION RATE OF LWR SPENT FUEL

W. J. Gray
L. E. Thomas
R. E. Einziger

November 1992

Presented at the
Materials Research Society
16th International Symposium
on the Scientific Basis for
Nuclear Waste Management
November 30 - December 4, 1992
Boston, Massachusetts

Prepared for
the U.S. Department of Energy
under Contract DE-AC06-76RLO 1830

Pacific Northwest Laboratory
Richland, Washington 99352

# EFFECTS OF AIR OXIDATION ON THE DISSOLUTION RATE OF LWR SPENT FUEL

W. J. Gray, L. E. Thomas, and R. E. Einziger
Pacific Northwest Laboratory, P.O. Box 999, Richland, WA 99352

## ABSTRACT

Dissolution rates for air-oxidized spent fuel were measured in flowthrough tests. Results from two types of specimens, separated grains and multigrain particles, both in oxidized ($U_4O_{9+x}$) and unoxidized ($UO_2$) conditions indicated only minor effects of oxidation on the surface-area-normalized rates. Similar results were obtained for unirradiated specimens in three different oxidation states ($UO_2$, $U_3O_7$, and $U_3O_8$). These observations have important practical implications for disposal of spent fuel in a geologic repository as well as implications regarding the oxidative dissolution mechanism of $UO_2$ fuel.

## INTRODUCTION

Spent $UO_2$ fuel from light-water reactors (LWRs) is being evaluated as a waste form for disposal in a geologic repository. A major factor controlling the long-term rate of release of soluble radionuclides, such as $^{135}Cs$ and $^{99}Tc$, from a repository is the rate of dissolution of the $UO_2$ matrix [1,2]. Therefore, it is important to measure the rate of dissolution and determine how it is affected by water chemistry and by the physical and chemical conditions of the fuel itself.

One fuel condition that must be investigated is a higher oxidation state resulting from exposure to air at mildly elevated temperatures. Fuel oxidation could occur in a potential repository site at Yucca Mountain, Nevada, which is in the unsaturated zone above the water table and would be relatively dry. Contact of the fuel by liquid water would not be expected during the first several hundred years after disposal while waste package

temperatures exceed 95°C. If the waste container and fuel cladding both fail during that time period, the fuel could be exposed to air and become oxidized. Later, after the repository has cooled, the fuel could be contacted by water.

Oxidation of spent fuel could increase its dissolution rate in water either by increasing the chemical reaction rate of the fuel with water[(a)] or by increasing the surface area of the fuel as a result of oxidation-induced cracking of grain boundaries [3]. To explore the first possibility, single-grain specimens of preoxidized and unoxidized spent fuel were tested. This type of specimen eliminates the uncertainty in effective surface area that would be associated with partially exposed grain boundaries of multigrain specimens and thus allows surface-area-normalized chemical reaction rates to be determined. The second possibility was explored by testing multigrain specimens. If oxidation increased the effective surface area by cracking open the grain boundaries, multigrain specimens of preoxidized and unoxidized spent fuel would dissolve at different rates.

The preoxidized spent fuel used in these tests consisted of cubic $U_4O_9$ having a stoichiometry of $\sim UO_{2.4}$, hereafter designated $U_4O_{9+x}$. $U_4O_{9+x}$ of this stoichiometry is the normal product of oxidizing LWR spent fuel in air at 110 to 200°C [3]. In this temperature range, the $U_4O_{9+x}$ phase persists for long times as evidenced by the lack of $U_3O_8$ formation in tests conducted up to several years at 175° to 195°C. Limited kinetic data from spent fuel oxidation at higher temperatures indicate that the $U_3O_8$ formation could be suppressed up to several thousand years at 90°C. Preliminary studies, still

---

(a) Evidence to suggest this includes the observation that dissolution rates of both spent fuel and unirradiated $UO_2$ depend upon the dissolved oxygen concentration in water [4].

ongoing, indicate that $U_4O_{9+x}$ may be the stable state if the waste container and fuel cladding do not fail in a repository until the fuel temperature drops below 150°C [3].

In contrast to LWR spent fuel, air-oxidation of unirradiated $UO_2$ produces a different oxidation product, $U_3O_7$, which readily continues oxidizing to $U_3O_8$. Oxidation behavior intermediate between that of typical LWR fuel and unirradiated $UO_2$ might be expected in spent fuel having low burnups, i.e., $U_3O_7$ might form in low burnup fuels. Because no spent fuel in this oxidation state was available, unirradiated specimens with different oxidation conditions ($UO_2$, $U_3O_7$, and $U_3O_8$) were tested. Some of the results, which are included here for completeness, were described in an earlier paper [5].

## EXPERIMENTAL

The spent fuel specimens were prepared from a single batch of ATM-105 fuel.[(a)] Coarse particle specimens were prepared by crushing and screening (-10/+24 Tyler mesh) spent fuel fragments and oxidizing a portion of the particles at 175°C to ~$UO_{2.4}$ as determined by weight gain measurements [3]. Ceramographic and x-ray diffraction analyses showed that the material was $U_4O_{9+x}$ containing small $UO_2$ remnants (~1 to 5 vol%) at the grain centers, and no detectable $U_3O_8$ or other oxidation products. Specimens consisting of separated grains of both oxidized and unoxidized spent fuel were prepared by crushing the above particles causing them to fracture predominantly along grain boundaries [6]. All four of the specimen materials (oxidized and unoxidized particles and grains) were washed to remove the fines and thus

---

(a) Boiling-water reactor spent fuel discharged in 1982 from the Cooper Nuclear Power Plant.[7] The specimens used in this work were from Rod ADD2974, which had a peak burnup of 31 MWd/kgM and a fission gas release of 0.6%.

reduce uncertainties in the measured surface areas. Throughout this report, "particles" refers to specimens consisting of ~700- to 1700-$\mu$m particles, each particle containing several thousand 15- to 25-$\mu$m grains. "Grains" refers to specimens consisting of separated grains.

Surface areas of the oxidized and unoxidized spent fuel grain specimens were measured to be 910 and 980 $cm^2/g$, respectively [5]. For the particle specimens, the surface areas were measured by weighing representative particles and calculating their surface areas, assuming that the particles were cubes and ignoring the internal grain boundary surfaces. These calculated values were averaged and multiplied by surface roughness factors of three, as was done previously with the grain specimens, to yield values of 15 and 17 $cm^2/g$ for the oxidized and unoxidized specimens, respectively.

Unirradiated powder specimens (44 to 105 $\mu$m) were prepared by crushing and screening $UO_2$ pellets. Oxidation of a portion of this material for 94 h at 225°C produced a thin (1 to 2 $\mu$m) layer of $U_3O_7$ on the $UO_2$ particles. The surface areas of these specimens were 270 $cm^2/g$ [5]. Specimens of $U_3O_8$ were prepared by oxidizing a portion of the $UO_2$ powder in air at 340°C for 18 h. The resulting oxygen-to-metal ratio averaged 2.68 (based on weight gain and assuming the starting material was $UO_{2.00}$). This compares favorably with the stoichiometric $U_3O_8$ ratio of 2.67. X-ray diffraction analysis indicated that the resulting powder was 100% $U_3O_8$ to within the detection limits of the method (~1%). The surface area of the $U_3O_8$ powder, measured by the BET method, was 12,200 $cm^2/g$.

Dissolution rates of the spent fuel and unirradiated uranium oxide specimens were measured using a flowthrough system [6,8]. In each test, the specimen size and flow rate were adjusted to maintain the uranium

concentrations in the column effluent well below the uranium solubility limit. This ensured that the measured dissolution rates were unimpeded by solubility constraints. The systems were operated continuously with the column effluents normally disposed of in a waste stream. Periodically, samples of column effluent were collected and analyzed, and the results were used to calculate dissolution rates according to the following equation:

$$R_i = \frac{C_i F}{MAf_i}$$

where $R_i$ = dissolution rate of component i (U or Cs)

$C_i$ = concentration of component i in column effluent

F = flow rate of test solution through column

M = mass of test specimen

A = specific surface area of test specimen

$f_i$ = concentration of component i (U or Cs) in test specimen.

Dissolution rates calculated for different components using this equation are equal if the specimen dissolves congruently. Following the flowthrough tests, the spent fuel particle specimens were examined by optical ceramography and scanning electron microscopy (SEM) to determine the nature of the dissolution attack.

The results reported here involved three different test conditions, as shown in Table I. In each case, the objective was to compare dissolution rates of oxidized versus unoxidized specimens under identical test conditions. However, no direct comparison of dissolution rates obtained for the three different test conditions is possible.

TABLE I. List of Test Specimens and Associated Test Conditions

| | $[Na_2CO_3] + [NaHCO_3]$ (molar) | $O_2$ fugacity[(a)] (atm) | pH[(a,b)] | Temp. ±3°C |
|---|---|---|---|---|
| All spent fuel specimens | $2 \times 10^{-3}$ | 0.2 | 8.7 - 8.9 | 50 |
| Unirradiated $UO_2$ $U_3O_7$, and $U_3O_8$ | $2 \times 10^{-2}$ | 0.2 | 8.0 - 8.2 | 23 |
| Unirradiated $UO_2$ and $U_3O_7$ | $2 \times 10^{-4}$ | 0.002 | 9.7 - 10.2 | 23 |

(a) The water supply reservoirs were slowly and continuously sparged with gas containing appropriate concentrations of $O_2$ and $CO_2$, balance $N_2$, to fix the oxygen fugacity and stabilize the pH.
(b) pH was measured at room temperature and a calculated temperature correction was applied, where appropriate.

RESULTS

Figure 1 shows dissolution rates for all four spent fuel specimens. Nearly identical dissolution rates of both U and Cs are depicted in Figure 1a for the oxidized and unoxidized spent fuel grains [5]. Figure 1b shows that the U dissolution rates from the oxidized spent fuel particles were initially a little higher than from the unoxidized particles, but the difference was less than a factor of two and decreased with time. The Cs dissolution rates were about double the U dissolution rates for both the oxidized and unoxidized particle specimens.

Comparison of the U results in Figures 1a and 1b indicates that the dissolution of the particle specimens was 4 to 7 times faster than that of the grain specimens. This apparent difference is undoubtedly due to underestimation of the effective surface area of the particles at least partially as a result of grain boundary attack, as shown in Figure 2.

Figure 2 shows ceramographic micrographs of oxidized and unoxidized spent fuel particles after dissolution testing. The grain boundaries, which

are visible in cross section, were attacked to a depth of 2 to 3 grain diameters in both the oxidized and unoxidized specimens. This observation is consistent with the apparent differences in the U dissolution rates between the grain and particle specimens.

Figure 3 shows SEM micrographs of unoxidized spent fuel particle specimens before and after dissolution testing. SEM micrographs of oxidized particles (not shown) were indistinguishable from those of the unoxidized particles. The most distinctive feature of the particles after dissolution testing is the rough, worm-eaten appearance of the grain boundary surfaces. In contrast, the transgranular fracture surfaces, two of which are visible in Figure 3b, remained smooth after testing. This difference between inter- and transgranular fracture surfaces has been observed for numerous specimens, both from the current dissolution tests and from previous tests conducted under similar conditions. It may be that the difference is associated with the enrichment of fission products along grain boundaries, but the mechanism has not been determined.

Figure 4a shows the dissolution rate of unirradiated $U_3O_8$. For comparison, the dissolution rates of $UO_2$ and $U_3O_7$ are shown in Figure 4b [5]. Although the chemical dissolution rate of $U_3O_8$ (left scale) was only 2 to 4 times greater than those of $UO_2$ and $U_3O_7$, the difference in fractional rates (right scale) was a factor of 100 or more.[(a)] Thus, the data show that as $UO_2$ was air-oxidized to $U_3O_7$ and $U_3O_8$, the effect on the chemical dissolution rate was modest. However, the large increase in surface area upon formation of $U_3O_8$ resulted in a large increase in the fractional dissolution rate.

---

(a) The $U_3O_8$ test was terminated after 17 days because 30% of the specimen had dissolved by that time.

All the dissolution rates depicted in Figures 1 and 4 were from tests that involved air-saturated solutions in which the effect of air oxidation on subsequent chemical dissolution rates was shown to be small. In comparison, Figure 5 shows the dissolution rates of $UO_2$ and $U_3O_7$ in water with an oxygen fugacity of only 0.002 atm; i.e., 1% of air saturation. Even here, the difference between $UO_2$ and $U_3O_7$ was not large (initially a factor of about 4 and apparently decreasing with time), but it was somewhat larger than that measured in air-saturated water.

## DISCUSSION

### Effect of Grain Boundaries on Specimen Surface Areas

The difference in dissolution rates between grains and particles (Figures 1a and 1b) is consistent with partial grain boundary exposure shown for the particles in Figure 2. If the grain boundaries for just the outer layer of grains on each particle were penetrated by the water, the exposed surface area would be increased by a factor of roughly five[(a)] over the calculated value, which is enough to account for the observed difference in dissolution rates. However, dissolution from the confines of grain boundaries is likely to be slower than from free surfaces. Due to limited movement of the test solution within the grain boundaries, U concentrations may approach saturation, and transport of reacting species in and out of grain boundary regions may depend upon diffusion. Therefore, the actual depth of water penetration could reasonably be expected to be at least 2 or 3 grain layers, which is consistent with the observations in Figure 2.

---

(a) The increased surface area would be exactly a factor of five if the grains were cubical and the exposed surface increased from just the outer surface to the outer surface plus the four side surfaces.

While grain boundary attack is thought to be the major factor responsible for the larger surface area of the particle specimens compared to the grain specimens, there is a second possible reason for the difference between the two types of specimens. Namely, the particle surfaces (Figure 2a) may be somewhat rougher than those of the individual grains.

Effect of Oxidation on Dissolution Rates

Data shown in Figure 1a indicate that air oxidation had little effect on dissolution rates of both U and Cs from spent fuel grains. However, Figure 1b shows that air oxidation did produce a small increase in the dissolution rate of the particles, not quite doubling the short-term U rates and somewhat more than doubling the Cs rates. Dissolution rates of oxidized particles that are double those of the unoxidized particles would indicate that the effective surface area of the former was doubled, perhaps by increased depth of grain boundary attack. A greater depth of attack for the oxidized particle is not obvious in the ceramographs shown in Figure 2. However, due to expected particle-to-particle variations, several more cross-sectional examinations of oxidized and unoxidized particles would be required to determine whether, on average, the depth of grain boundary attack is greater for the oxidized particles. In any case, the effect of oxidation on dissolution rates and on the depth of grain boundary attack was relatively small considering the thousands of additional grain boundary surfaces that potentially could have been made accessible to the water.

Other Observations

Figure 1a shows that U and Cs dissolved nearly congruently (at equal normalized rates) from the fuel grain specimens, in agreement with data obtained earlier with different fuel grain specimens [6]. Not unexpectedly,

the Cs dissolution rates from the particles were about double the U dissolution rates (Figure 1b). Similar results have been reported for other spent fuel dissolution tests.[e.g., 1,9] This occurs when the test specimens consist of multigrain particles or fragments because Cs dissolves from grain boundaries where it is slightly enriched.

Figure 3b shows a very rough surface. All the intergranular fracture surfaces of spent fuel particles and grains that have been examined following flowthrough dissolution testing in bicarbonate solutions have this appearance. It would appear that the surface area should be increased by the formation of this surface layer and that the dissolution rates should be observed to increase with time as this layer is formed. However, while an increasing rate is sometimes found (e.g., Figure 5), it is more common to find a decrease in dissolution rate with time. Further work will be required to determine the nature of these surface layers and how they are produced by the dissolution process.

Mechanistic Implications

Data presented in this paper also have important implications regarding the mechanism of spent fuel oxidation/dissolution. A valid oxidation/dissolution model must be able to explain why air oxidation of either irradiated fuel to $U_4O_{9+x}$ or unirradiated $UO_2$ to $U_3O_7$ has little effect on subsequent chemical dissolution rates, even in partially anoxic water. There are at least two possible explanations: 1) the oxidized surface formed in air is different from that formed in oxygenated water; or 2) there are at least two oxidation steps involved in the dissolution mechanism, one of which is rate limiting. If the first postulate applies, an additional oxidized (or hydrated) layer must still be formed in the water, even though the specimen

had previously been air oxidized to $U_4O_{9+x}$ or $U_3O_7$. If the second explanation has validity, then the aqueous formation of an oxidized layer on a previously unoxidized surface must be a rapid, non-rate-limiting step, and there must be a subsequent rate limiting step involving dissolved oxygen. In either scenario, prior formation by air oxidation of an oxidized phase ($U_4O_{9+x}$ or $U_3O_7$) on the surface of irradiated or unirradiated fuel would have no effect on subsequent dissolution rates, in agreement with observations.

FUTURE WORK

Data presented in Figure 4 show that the formation of $U_3O_8$ would result in a large increase in total (fractional) dissolution rate, primarily due to the large increase in surface area. Therefore, an important next step in the oxidation studies will be to determine whether conditions in a potential Yucca Mountain repository can promote the oxidation of spent fuel to the $U_3O_8$ state. Previous oxidation tests conducted with LWR spent fuel indicate that the fuel can be oxidized beyond $U_4O_{9+x}$ to $U_3O_8$ [10]. However, the temperatures needed to observe this reaction on a laboratory time scale are considerably higher than those envisioned for a repository.

Low-burnup spent fuel may oxidize to form $U_3O_7$ as suggested in the introduction. However, even if a $U_3O_7$ product similar to that obtained from oxidation of unirradiated $UO_2$ resulted from oxidation of a low-burnup fuel, data presented in Figures 4 and 5 indicate that the formation of $U_3O_7$ would have little effect on the fuel dissolution rates.

Assuming that repository conditions can be tailored to preclude the formation of $U_3O_8$, additional tests will be required to determine whether the results presented here for $U_4O_{9+x}$ and $U_3O_7$ can be generally applied to spent fuel that may be placed in a repository. In addition, the dissolution rates

of spent fuel and its oxidation products must be compared under additional water chemistry conditions that encompass those expected in a repository.

## CONCLUSIONS

Data presented in this paper provide partial answers to three important questions regarding the possible behavior of spent fuel in a potential Yucca Mountain repository. Under the limited conditions tested, 1) air oxidation of spent fuel to $U_4O_{9+x}$ ($UO_{2.4}$) had no appreciable effect on chemical dissolution rates in air-saturated solutions, 2) air oxidation of fuel to $U_4O_{9+x}$ slightly increased its effective surface area but, from a repository standpoint, the associated increase in dissolution rate was relatively small, and 3) if the fuel were oxidized to $U_3O_8$, a large increase in dissolution rate would result, primarily from the increase in fuel surface area.

## ACKNOWLEDGMENTS

This work was performed at Pacific Northwest Laboratory (PNL) with U.S. Department of Energy (USDOE) funding through Lawrence Livermore National Laboratory in support of the Yucca Mountain Site Characterization Project (YMP) as part of the Civilian Radioactive Waste Management Program. The YMP is managed by the YMP office of the USDOE, Las Vegas, Nevada. PNL is operated for the USDOE by Battelle Memorial Institute under Contract DE-AC06-76RLO 1830.

## REFERENCES

1. L. H. Johnson, N. C. Garisto, and S. Stroes-Gascoyne in Waste Management '85, Vol. 1--High-Level Waste, edited by R. G. Post (Proceedings of the Symposium on Waste Management at Tucson, Arizona, March 24-28, 1985), pp. 479-482.

2. M. J. Apted, A. M. Liebetrau, and D. W. Engel in Waste Management '87, Vol 2--High-Level Waste, edited by R. G. Post (Proceedings of the Symposium on Waste Management at Tucson, Arizona, March 1-5, 1987), pp. 545-554.

3. R. E. Einziger, L. E. Thomas, H. C. Buchanan, and R. B. Stout, J. Nucl. Mater. 190, 53 (1992).

4. L. H. Johnson and D. W. Shoesmith, "Spent Fuel," Chapter 11 in Radioactive Waste Forms for the Future, edited by W. Lutze and R. C. Ewing (North-Holland Publishers, New York, 1988).

5. W. J. Gray and L. E. Thomas in High Level Radioactive Waste Management, Proceedings of the Third International Conference, (American Nuclear Society, Inc., La Grange Park, IL, 1992), Vol. 2, pp. 1458-1464.

6. W. J. Gray and D. M. Strachan in Scientific Basis for Nuclear Waste Management XIV, edited by T. Abrajano, Jr. and L. H. Johnson (Materials Research Society, Pittsburgh, PA, 1991), Vol. 212, p. 205.

7. R. J. Guenther et al., Characterization of Spent Fuel Approved Testing Material - ATM-105, PNL-5109-105 (Pacific Northwest Laboratory, Richland, WA, 1989).

8. C. N. Wilson and W. J. Gray in High Level Radioactive Waste Management (American Nuclear Society, Inc., La Grange Park, IL, 1990), Vol. 2, pp. 1431-1436.

9. Y. B. Katayama, D. J. Bradley, and C. O. Harvey, Status Report on LWR Spent Fuel IAEA Leach Tests, PNL-3173 (Pacific Northwest Laboratory, Richland, WA, 1980).

10. R. E. Einziger and R. V. Strain, Nucl. Tech. 75, 82 (1986).

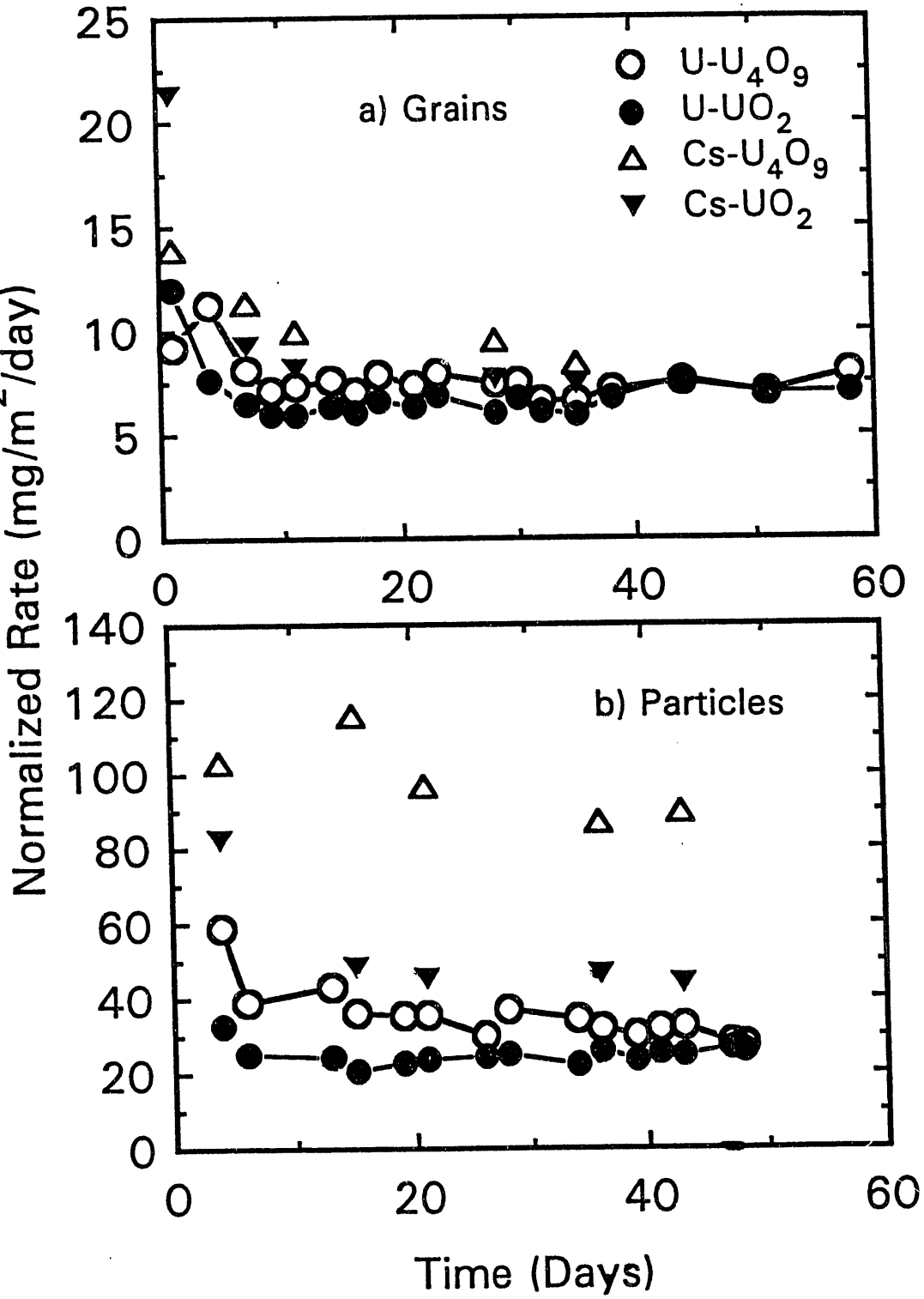


Figure 1. Dissolution rates from spent fuel in 2 x $10^{-3}$ M $NaHCO_3/Na_2CO_3$ solution at 50 ±2°C, pH = 8.8 to 9.0, 0.2 atm $O_2$ partial pressure. Legend applies to both figures: a) grains; b) particles.

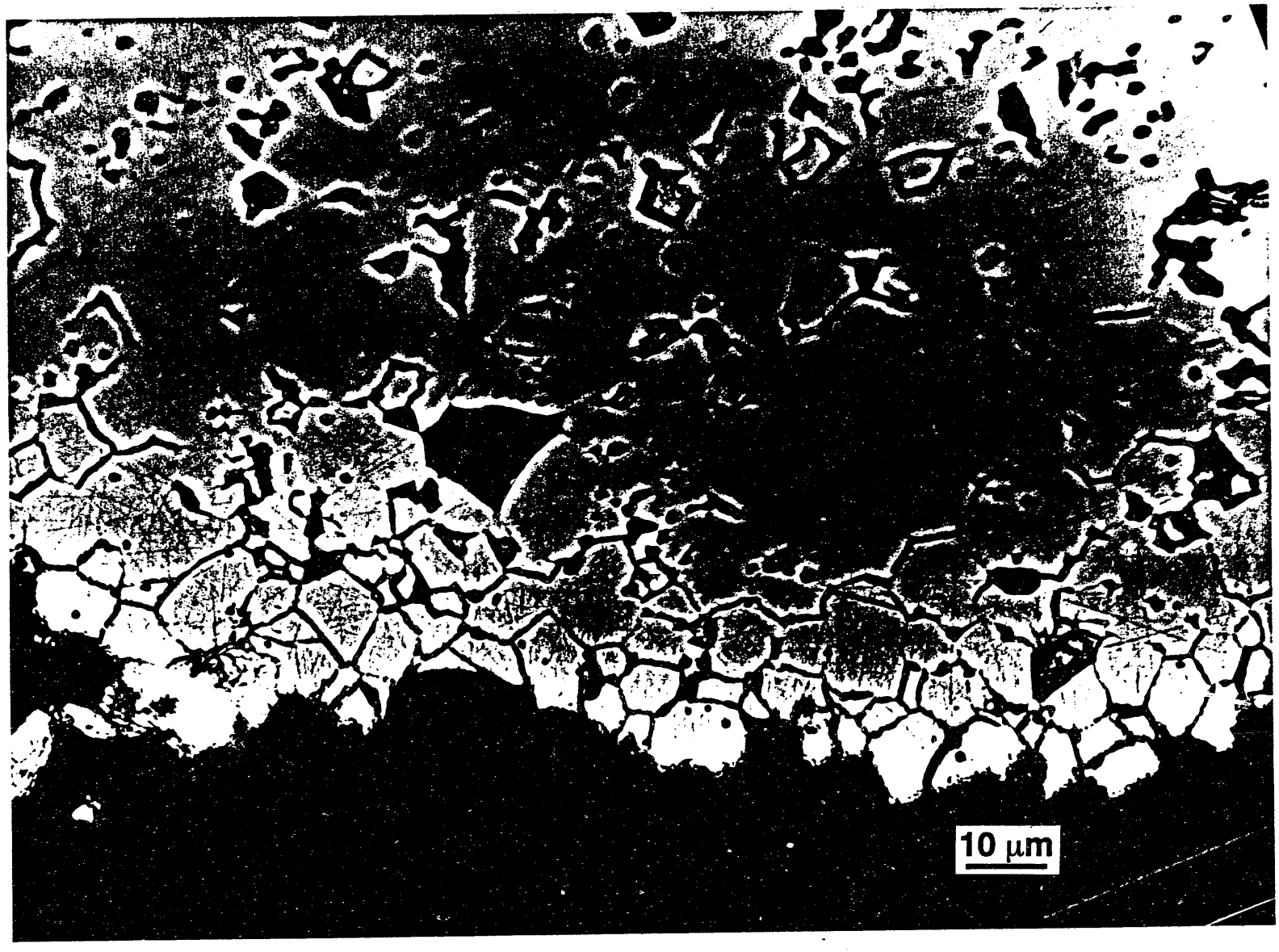


Figure 2a. Ceramograph of unoxidized spent fuel particle following dissolution testing shown in Figure 1b.

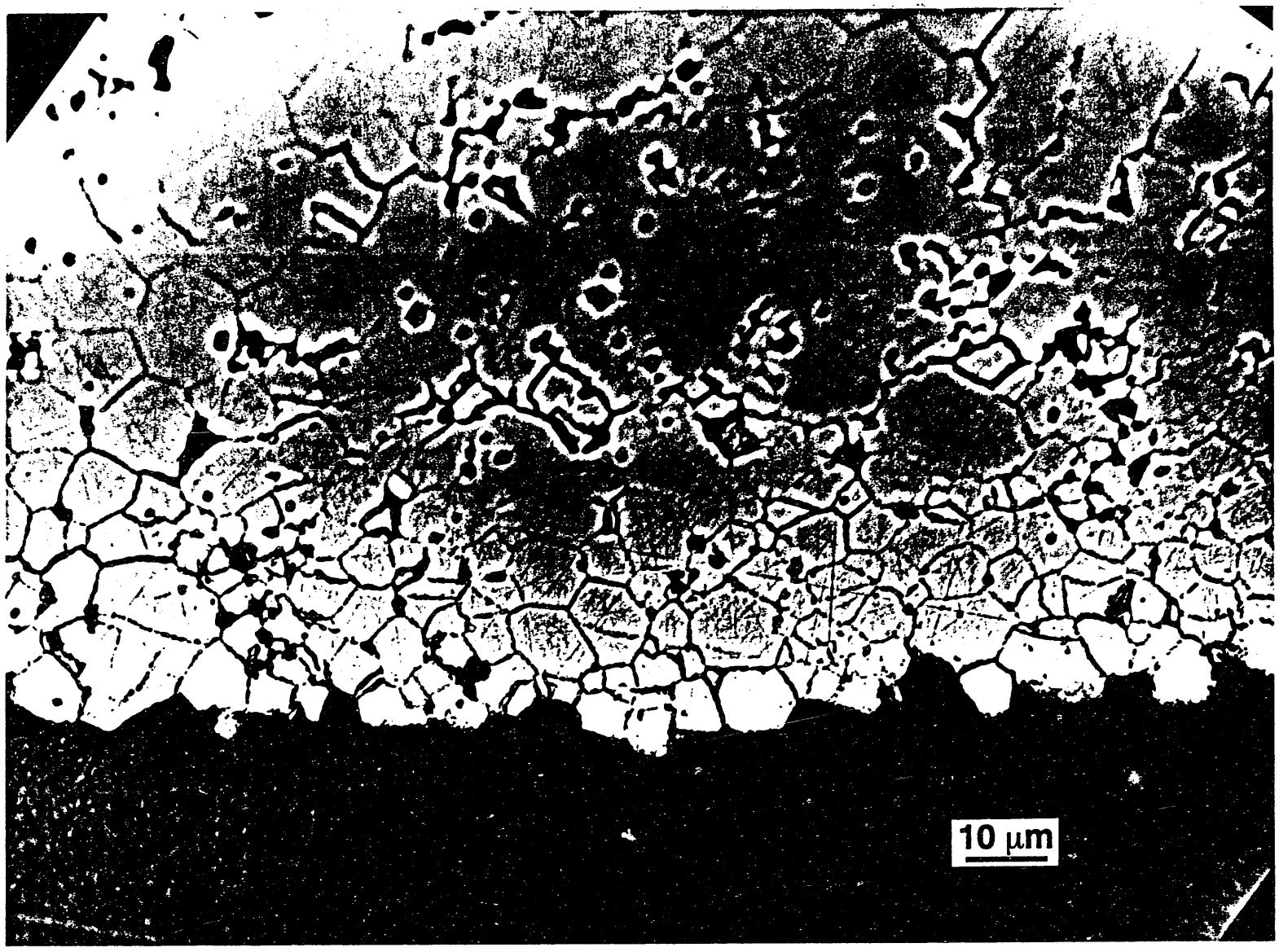


Figure 2b. Ceramograph of oxidized spent fuel particle following dissolution testing shown in Figure 1b.

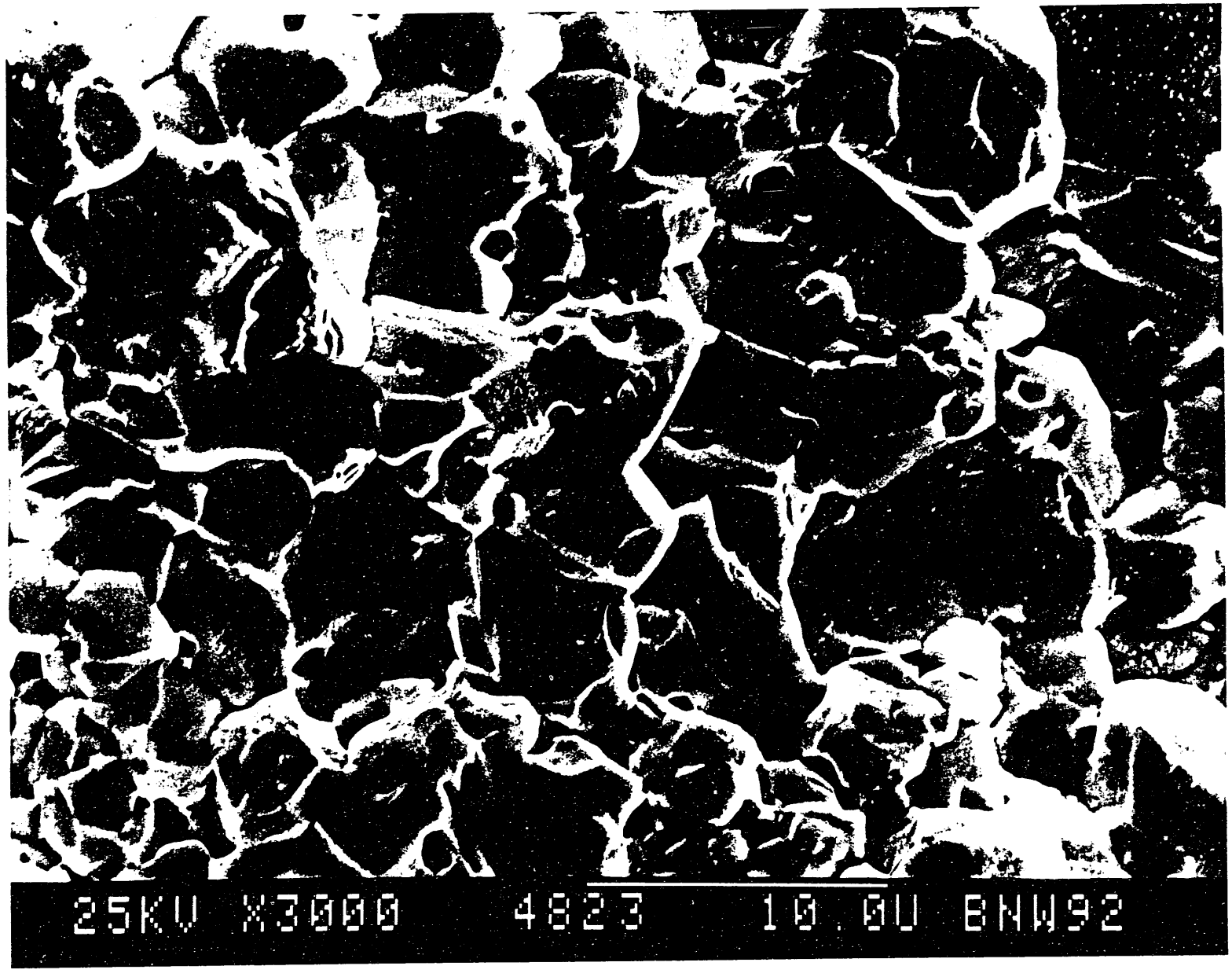


Figure 3a. SEM photograph of unoxidized spent fuel particle prior to dissolution testing.


Figure 3b. SEM photograph of unoxidized spent fuel particle after dissolution testing shown in Figure 1b.

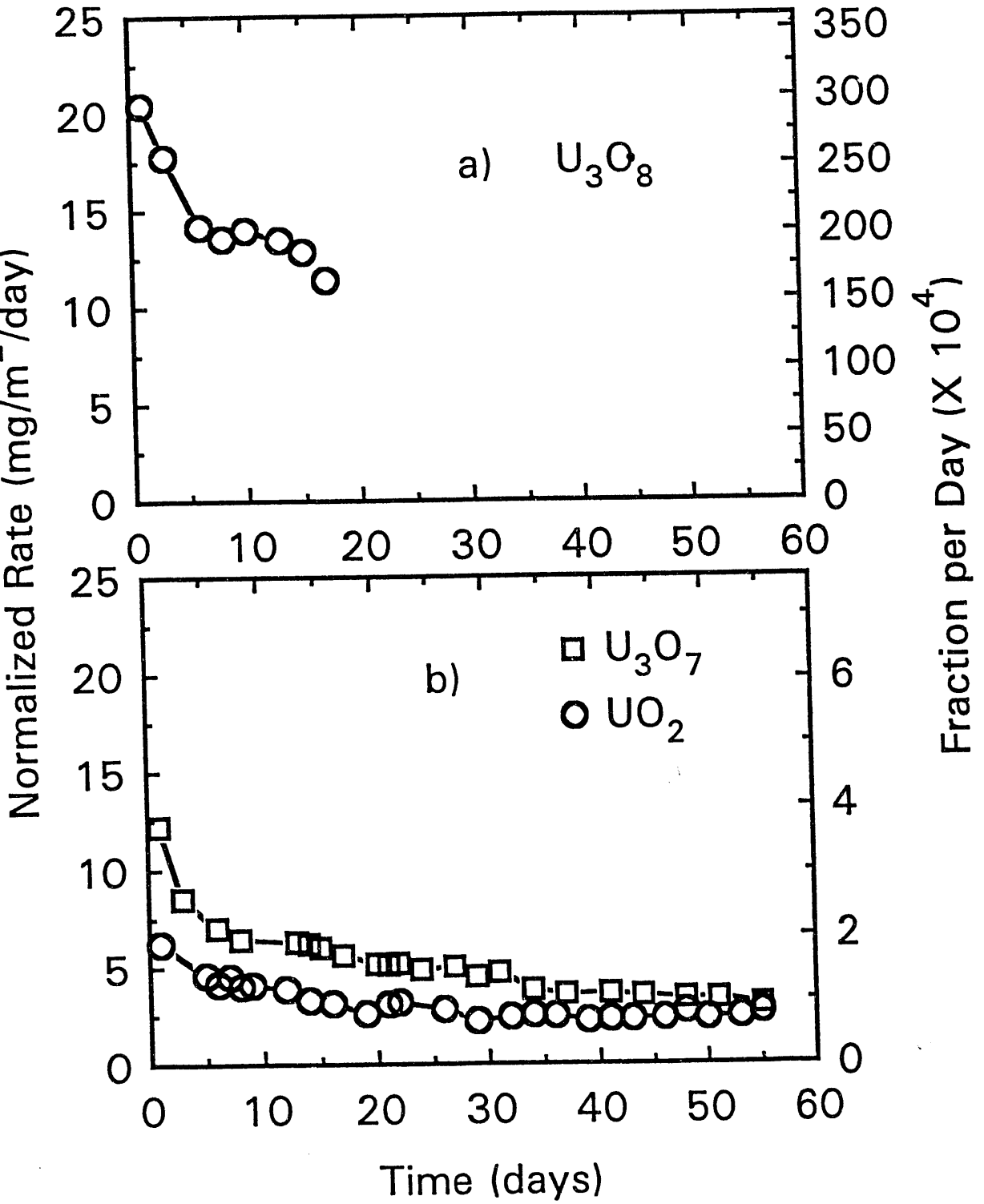


Figure 4. Dissolution rate of unirradiated specimens in 2 x $10^{-2}$ M $NaHCO_3$ solution at room temperature (~25°C), pH = 7.9 to 8.1, 0.2 atm $O_2$ partial pressure.

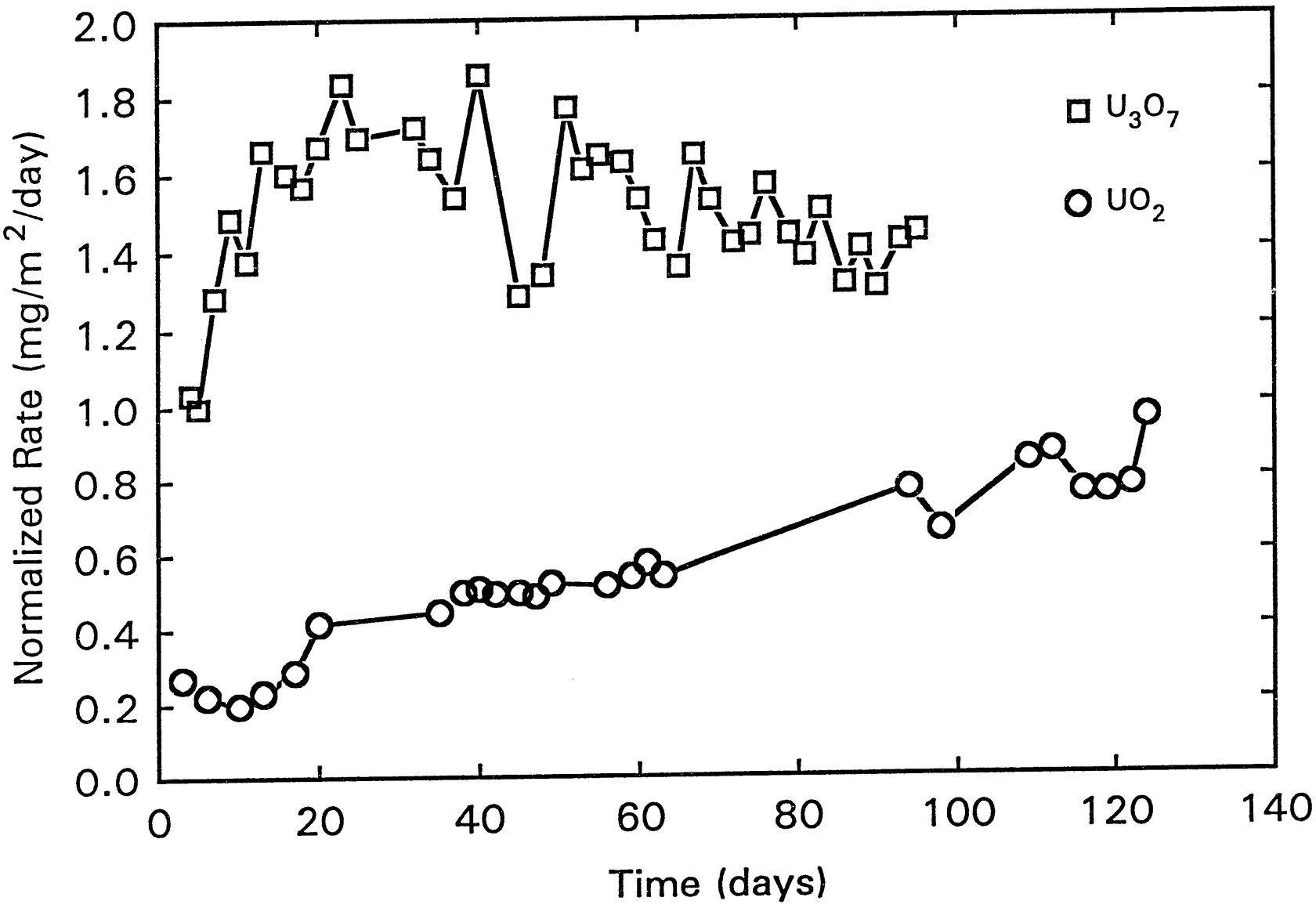


Figure 5. Dissolution rate of unirradiated specimens in 2 x $10^{-4}$ M $Na_2CO_3$ solution at room temperature (~25°C), pH = 9.9 to 10.1, 0.002 atm $O_2$ partial pressure.

# END

# DATE FILMED

3/18/93